Volume 265, Issues 3–4 30 January 2008 ISSN 0012-821X

ELSEVIER

EARTH & PLANETARY SCIENCE LETTERS

Available online at www.sciencedirect.com
ScienceDirect
Earth and Planetary Science Letters 265 (2008) 386–395
EPSL
www.elsevier.com/locate/epsl

Possible chemical modification of oceanic lithosphere by hotspot magmatism: Seismic evidence from the junction of Ninetyeast Ridge and the Sumatra–Andaman arc

Meghan S. Miller *, Cin-Ty A. Lee [1]

Rice University, Department of Earth Science, 6100 Main St. MS 126, Houston, TX, USA 77005

Received 14 May 2007; received in revised form 9 October 2007; accepted 16 October 2007
Available online 30 October 2007
Editor: R.W. Carlson

Abstract

Tomograms of the upper mantle, which represent perturbations in P-wave, shear wave speed, and bulk-sound speed, image the Indo-Australian plate subducting beneath the Eurasian plate along the Sumatra–Andaman arc. The detailed images of the subducting slab are well constrained by the large number of intermediate depth earthquakes and moderate seismic station coverage along the entire Indonesian–Sumatra–Andaman arc. The steeply dipping slab is coherent, defined by seismicity and higher velocity perturbations, beneath the entire arc, but at approximately 9.5–12.5 °N and at 60–160 km depth, the slab is characterized by a low P-wave signal, with only a small decrease in the S-wave speed, and a modest decrease in bulk-sound speed. At this position along the arc the inactive Ninetyeast Ridge, suggested to be a plume-fed spreading ridge, is being subducted beneath the Andaman Islands. The negative P-wave and bulk-sound speed anomalies in the slab, along with only a small decrease in S-wave speed cannot be explained by thermal variations alone and hence suggest a possible change in composition. We find that the seismic anomalies in this region of the slab are best fit by orthopyroxene-rich zones within the peridotitic lithospheric mantle. If correct, we speculate that these pyroxene-rich lithologies formed by the interaction of upwelling magmas with preexisting oceanic lithospheric mantle beneath the Ninetyeast Ridge before subduction. Our observations represent one of few seismic evidences for extensive chemical modification of lithospheric mantle.

Keywords: Sumatra–Andaman arc; tomography; chemical modification; Ninetyeast Ridge

1. Introduction

The lithospheric mantle underlying ocean basins and continents is mostly composed of fertile to depleted peridotites, representing the solid residues after melts were extracted to form the overlying crust. However, there is growing evidence from the studies of mantle xenoliths and exhumed mantle blocks (abyssal peridotites and

* Corresponding author. Tel.: +1 713 348 4286; fax: +1 713 348 3062.
E-mail addresses: meghan.s.miller@rice.edu (M.S. Miller), ctlee@rice.edu (C.-T.A. Lee).
[1] Tel.: +1 713 348 5084; fax: +1 713 348 3062.

0012-821X/$ - see front matter © 2007 Elsevier B.V. All rights reserved.
doi:10.1016/j.epsl.2007.10.039

ophiolites) that some parts of the lithospheric mantle have been subsequently modified by the passage of magmas (Kelemen et al., 1992, 1998; Liu et al., 2005). For example, pyroxene-rich zones in ophiolites, subarc mantle, and cratonic mantle, have been suggested to reflect reaction of residual peridotites with infiltrating pyroxene-saturated magmas. This type of chemical modification, if extensive, could significantly transform the physical properties of the lithospheric mantle. In particular, because pyroxene is much denser than olivine, a modal increase in pyroxene could provide a compositional-induced buoyancy force that eventually destabilizes the modified portion of the lithospheric mantle. This may be one additional means, besides subduction, by which lithospheric mantle is recycled back into the Earth's deep interior.

The problem, however, is that although these petrologic and field studies are numerous, their sampling lengthscales are small. These studies thus show that chemical modification by "secondary" processes happens (e.g., melt–rock reaction, diking, etc.) but they certainly do not constrain whether significant (on the scale of 10 km or more) amounts of lithosphere are actually affected. Seismology may be the best way to fully assess the extent of these processes. However, there are few earthquakes and seismometers in ocean basins. Even where there are seismometers, such as on hotspot volcanoes or volcanic arcs, the presence of melt masks the seismic signature of the melt–rock reaction products (Wagner et al., 2005; Wagner and Grove, 1998b). We are also not aware of melt–rock reaction zones being seen in seismic studies of cratons even though their existence is seen in the xenolith suites (Boyd, 1989). However, the lack of seismic evidence could simply be because the structure within cratonic mantle is too complicated (Fouch et al., 2004; James et al., 2001).

Here, we present tomographic images of the Sumatra–Andaman arc, where the Indo-Australian plate is subducting beneath the Eurasian plate (Fig. 1). It is here that the inactive northern extension of the Ninetyeast Ridge, a plume-fed spreading ridge (Saunders et al., 1991; Sclater and Fisher, 1974; Souriau, 1981), is being subducted and where we find unusual seismic velocity anomalies in the subducting slab. These seismic velocity anomalies are best explained by orthopyroxene-rich lithologies. We interpret these pyroxene-rich lithologies to have formed by the interaction of upwelling magmas with preexisting oceanic lithosphere beneath the Ninetyeast Ridge, which if correct, provide seismic evidence for extensive chemical modification of lithospheric mantle.

2. Tomographic images

Seismic properties of extinct ridges are difficult to image due to poor ray-path coverage and large tomographic cell sizes for the lithosphere and regions of interest. Here we have a unique opportunity to image oceanic lithosphere that has been altered by a plume-fed spreading ridge. Tomographic images of the Sumatra–Andaman subduction zone were created with the adaptation of a 3D ray tracing technique as part of a larger study that previously published the bulk-sound speed and shear wave-speed inversions, which focused on the joint inversion methodology and physical differences between slab that penetrate into the lower mantle and those that flatten in the transition zone (Gorbatov and Kennett, 2003).

Gorbatov and Kennett (2003) used an updated seismicity catalogue (Engdahl et al., 1998), parameterized the study region with 0.5° by 0.5° cells and varying thickness to 1500 km depth within a larger, surrounding model space which has 5° by 5° cells and 16 layers between the surface and the core–mantle boundary. A simultaneous inversion was made for both regional and global structures to minimize the influence of structures surrounding the Western Pacific region referenced to the

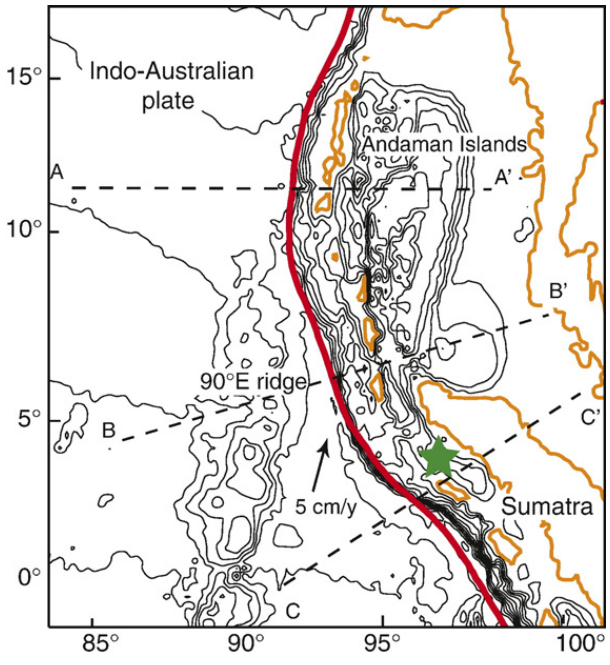

Fig. 1. Map of the Andaman–Sumatra arc region. The epicenter of 26 December 2004 Great Sumatra–Andaman earthquake is represented by a green star, the red line indicates the convergent plate boundary, and the dotted lines indicate the location of the cross sections in Fig. 3. Bathymetry from the ETOPO2 model with 1 km contours. (For interpretation of the references to colour in this figure legend, the reader is referred to the web version of this article.)

ak135 model (Kennett et al., 1995). The nested iterative approach applied 3-D ray tracing to account for the influence of three-dimensional variations of Earth structure between source and receiver. Only P and S readings from the Engdahl et al. (1998) catalogue with common source and receiver pairs were selected to ensure a close match between both P and S wave ray paths within the study area. This criterion also improved the location accuracy, improved the resolution of the structures and noise reduction, and in turn, this optimized data coverage ensured that the final images could be directly compared. Further description on the technique of joint bulk-sound and shear wave tomography can be found in Kennett et al. (1998). More details about the application of 3-D ray tracing are discussed in Gorbatov and Kennett (2003); Koketsu and Sekine (1998).

After the completion of the bulk-sound and shear wave-speed inversions (Gorbatov and Kennett, 2003), the same ray-path dataset and methodology was employed to yield a new P-wave inversion, in which a subset of the model was introduced in Miller et al. (2005, 2006). As previously described, joint tomographic inversion arrival times can provide insight into the physical properties of subducting slabs (Gorbatov and Kennett, 2003; Miller et al., 2005). The resulting images of bulk-sound and S-wave speed variation provide a separation of bulk and shear moduli, therefore a more direct comparison of mineral physics and petrologic information. For isotropic media the dependency on the shear modulus, μ, and the bulk modulus, κ, can be isolated. The bulk-sound speed, ϕ, was derived from the combination of S-wave speed (V_S), and P-wave speed (V_P) where

$$V_S = \sqrt{\frac{\mu}{\rho}} \text{ and } V_P = \sqrt{\frac{\kappa + 4/3\mu}{\rho}}, \text{ therefore}$$

$$\phi = \sqrt{V_P^2 - 4/3V_S^2} = \sqrt{\frac{\kappa}{\rho}}.$$

As a result, the relative variation in wave speeds depends on the variations in moduli and density. But if there are only variations in density, the local variations in wave speed are identical.

3. Seismic anomalies

All three tomographic models are shown in map view in Fig. 2 which depicts the subducting Indo-Australian plate, and its dramatic variation in physical properties, beneath the Andaman–Sumatra arc as a depth slices at 50 km and 125 km. Fig. 3 shows three profiles through each of the models along the three separate traverses (Fig. 1). The subducting Indo-Australian plate is imaged by coherent high wave speeds along the length of the arc, but there is a distinct change in the structure of along A–A'. Between 9.5–12.5 °N the high velocity anomalies associated with the subducting slab decrease in amplitude and change to relatively low P-wave (−0.6 to −0.2%) in the region where one should expect the slab to be present (60–160 km depth), yet there is no decrease in the S-wave speed (0.3 to 0.5%) and only small decrease in velocity perturbations in bulk-sound speed (−0.0 to −0.4%) (Fig. 3). Along this section of the arc, the Ninetyeast ridge collides with the Sumatra–Andaman arc and is subducted (Fig. 1). Checkerboard tests to assess the resolution of the images were performed and published in previous work (Gorbatov and Kennett, 2003) and it was concluded that the entire slab could be recovered using the same inversion parameters as in the observed data. In addition, we have mapped the ray-path coverage for both P- and S-waves for the Sumatra–Andaman arc and displayed the results in cross sections through A–A' and as slices at 100 km depth (Fig. 4). The results of these calculations and by estimating the size of the anomaly is roughly 3 times the grid size (0.5°), we can conclude that the anomaly is a real feature and not an artifact due to of lack of data coverage or resolution.

The seismic perturbations surrounding the anomalous area (Figs. 2 and 3) appear to be representative of the subducting Indo-Australian slab, as high wave speed perturbations (blue in the figures). These higher wave speeds can be explained by the fact that subducting oceanic lithosphere is colder than the surrounding mantle. The anomalous area has lower wave speeds than the surrounding slab. The entire subducted plate should have the same temperature at that depth (60–160 km), since both the ocean floor and the ridge are approximately Cretaceous in age (Müller et al., 1997). The presence of negative P-wave and bulk-sound anomalies in the slab with only a very small anomaly in S-wave (−0.1 to 0.2% decrease) cannot be explained by a hot temperature anomaly because increasing temperature results in a slightly larger proportional drop in S-wave than in P-wave speed. This can be seen in Fig. 5 using calculations based on Hacker and Abers, (2004) and Lee (2003). Therefore, the anomalous seismic velocities cannot be solely explained by temperature variations in the slab.

4. Possible scenarios for compositional modification

In this section, we explore compositional variations as the cause of the seismic velocity anomalies in the region where the Ninetyeast Ridge is being subducted.

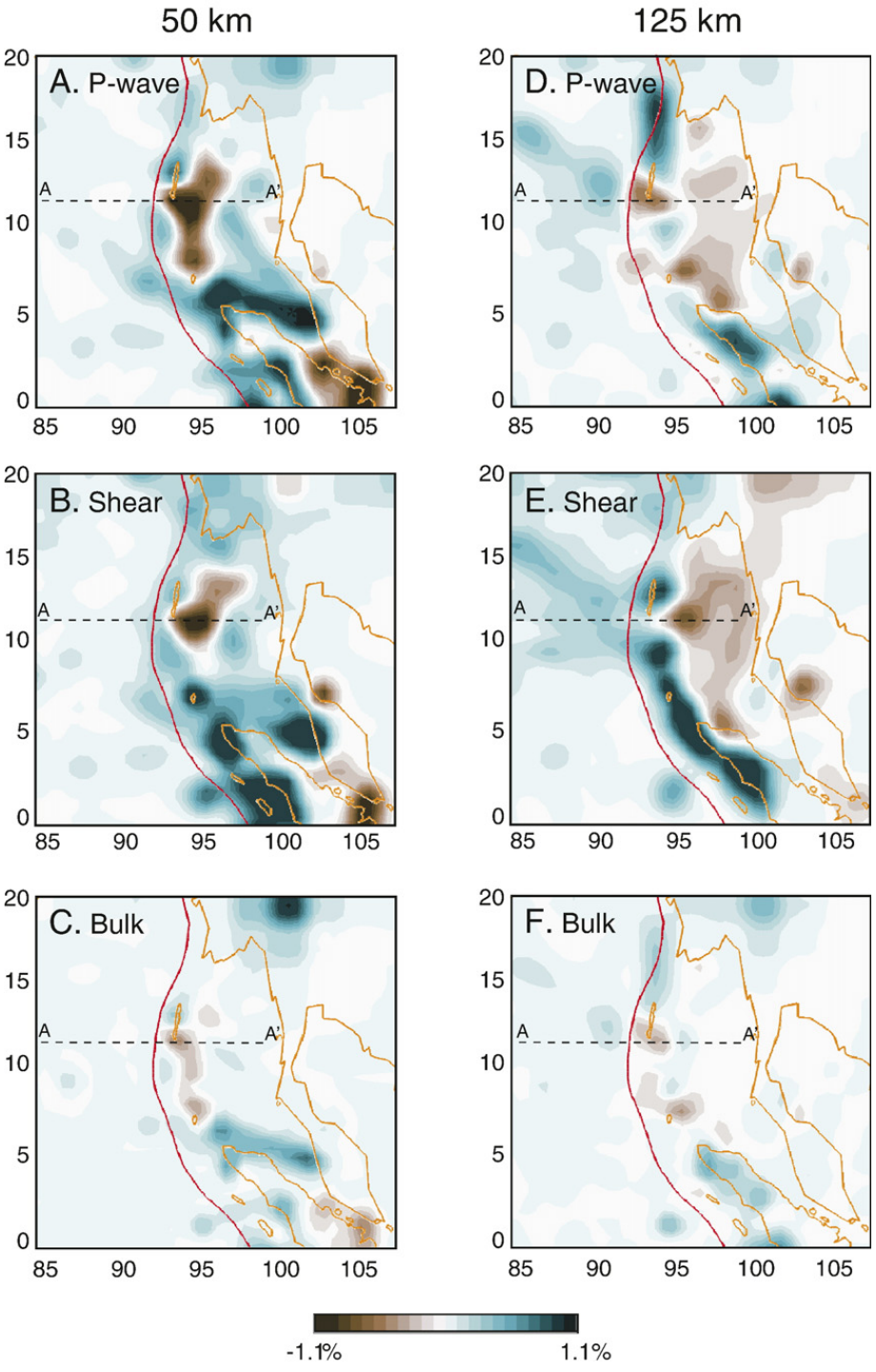

Fig. 2. Map views of the (A and D) P-wave, (B and E) S-wave, and (C and F) bulk sound speed tomographic models in the Sumatra–Andaman arc region for depths at 50 and 125 km. The red line indicates the convergent plate boundary and the orange lines represent the coastline. The blue color-filled contours represent fast velocity perturbations relative to the *ak135* reference model (Kennett et al., 1995) and the brown colors represent slow velocity perturbations.

One possibility for generating low velocity anomalies is to increase Fe content. However, this cannot explain the combined sense of these anomalies because a greater negative S-wave anomaly than P-wave anomaly would be predicted (Lee, 2003). This leaves us with the option of a mineralogic change. One constraint we have is the lack of a S-wave anomaly, which requires that the relative change in density and shear modulus are similar ($\delta\rho/\rho \sim \delta\mu/\mu$) at a given depth. This in turn implies that the change in bulk modulus, κ, and shear modulus, μ,

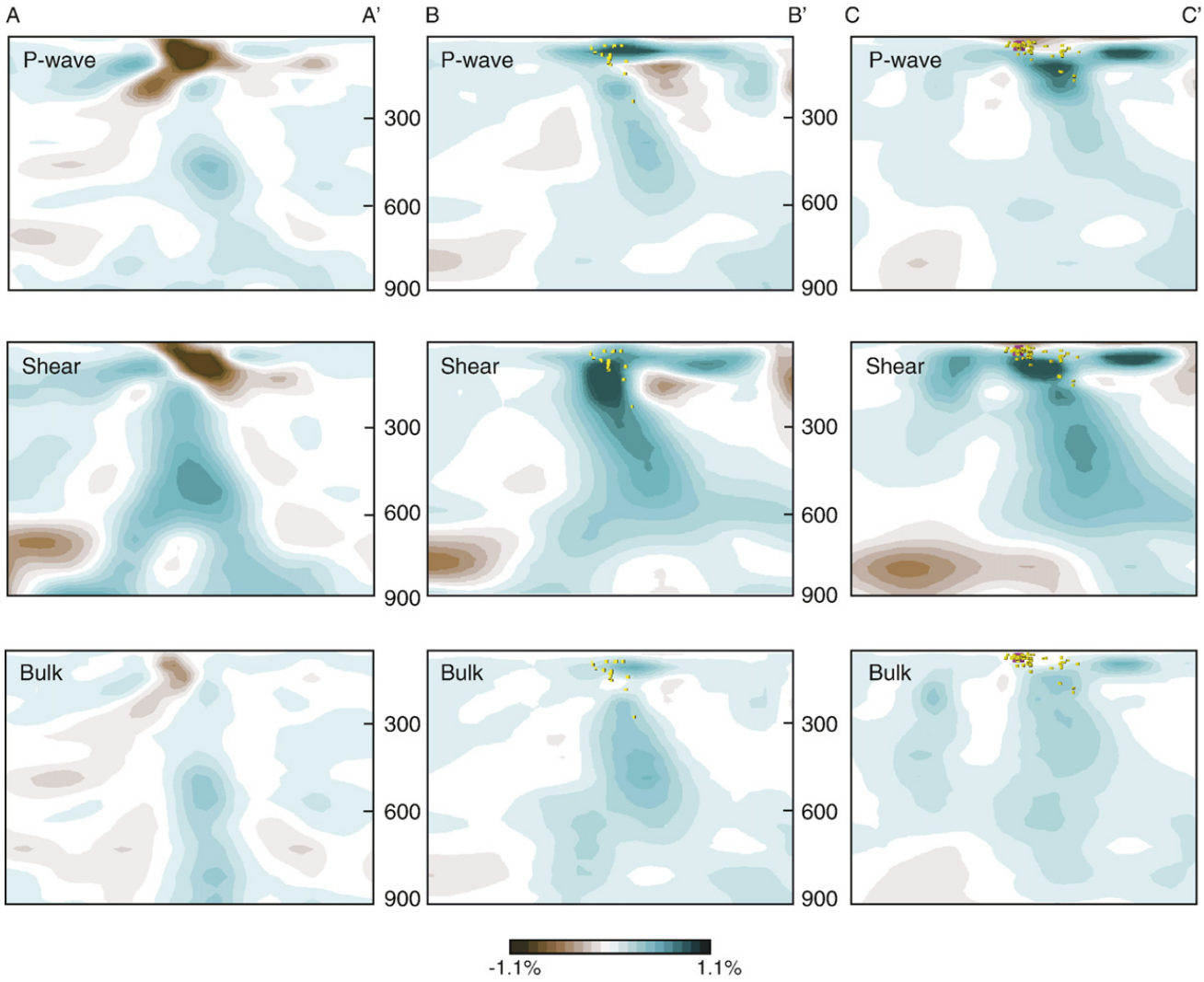

Fig. 3. Cross sections through the P-wave, S-wave, and bulk-sound speed tomographic models at the location shown in Fig. 1. A–A' is located where the Ninetyeast Ridge is subducting along the Sumatra–Andaman arc. The blue color-filled contours represent fast velocity perturbations relative to the *ak135* reference model (Kennett et al., 1995) and the brown colors represent slow velocity perturbations. The yellow dots indicate hypocenters from the Engdahl et al. (1995) catalogue and the pink square is the location of the Great Sumatra–Andaman earthquake mainshock.

between the anomalous zone and surrounding slab must satisfy the following requirement $\delta\kappa/\kappa < \delta\mu/\mu$.

Assuming that the reference slab is made largely of lherzolitic peridotite (Fig. 5), a number of scenarios are possible. An increase in the modal proportion of orthopyroxene (Fig. 5) relative to olivine satisfies this condition because the bulk modulus of orthopyroxene is significantly lower than that of olivine, whereas its shear modulus is only slightly lower than that of olivine (Bass, 1995; Chai et al., 1997). This condition still holds even at uppermost mantle pressures after the high pressure derivative of the bulk modulus (Chai et al., 1997) for orthopyroxene is considered. Other minerals that we might consider include clinopyroxene and garnet. Increased clinopyroxene mode causes a greater decrease in S- than in P-wave speeds, while increased garnet mode yields both positive P- and S-wave anomalies. A decrease, however, in clinopyroxene mode relative to a lherzolitic starting composition results in a greater decrease in P than S. Thus, it can be seen that orthopyroxene-rich harzburgites (olivine+orthopyroxene) have the appropriate P- and S-wave wave speed anomalies relative to lherzolite to match the observed seismic perturbations. Clinopyroxene-rich peridotites (such as olivine clinopyroxenites and wehrlites; Fig. 5) do not match observations.

We can also consider a reference slab with an eclogitic composition made up largely of clinopyroxene and garnet in subequal proportions. In this case, the anomalous zone is composed of peridotite, e.g., a "peridotite hole" within an eclogitized slab. However, this scenario is unlikely because although eclogites have

higher P-wave speeds than peridotite, they have lower S-wave signals due to the low S-wave speed of clinopyroxene (Horodyskyj et al., 2007). In addition, for this scenario to be correct, we would have to envision a subducting lithosphere that is entirely eclogite save for the peridotitic hole. As only the crustal part of the subducting lithosphere is expected to be eclogite (the remaining part of the lithosphere, the lithospheric mantle, is expected to be peridotite), this scenario seems highly unlikely.

Of the various hypotheses entertained, the most promising explanation for the seismically anomalous region appears to be orthopyroxene enrichment and clinopyroxene-depletion. Fig. 5 suggests that the seismically anomalous region observed in this study represents orthopyroxene-rich harzburgite. Such lithologies cannot be formed by melt depletion as extraction of melt leads to olivine-rich residues (see red arrow in Fig. 5C), hence, the enrichment in orthopyroxene suggests a secondary origin. As far as we know, our study is one of very few seismic studies to have shown evidence for orthopyroxene enrichment. Another report of orthopyroxene-rich zones, based on similar P- and S-wave speed perturbations, was proposed for the mantle wedge beneath the Andes in South America (Wagner et al., 2005).

5. Speculations

There are two ways to generate orthopyroxene enrichment in the mantle. One way is to generate SiO_2-rich melts by partial melting of basalt. As these silicic melts rise upwards, they would react with peridotite (Kelemen, 1995, 1998; Liu et al., 2005; Rapp et al., 1999). Due to their high SiO_2 contents, they would be saturated in orthopyroxene but not olivine so that melt–rock reaction would result in the conversion of any wall–rock olivine into orthopyroxene. This process has been suggested to occur in the mantle wedge of hot subducting slabs, in which the temperatures are hot enough to melt the oceanic crust (Drummond et al., 1996; Rapp et al., 1999). Such a process may be responsible for making

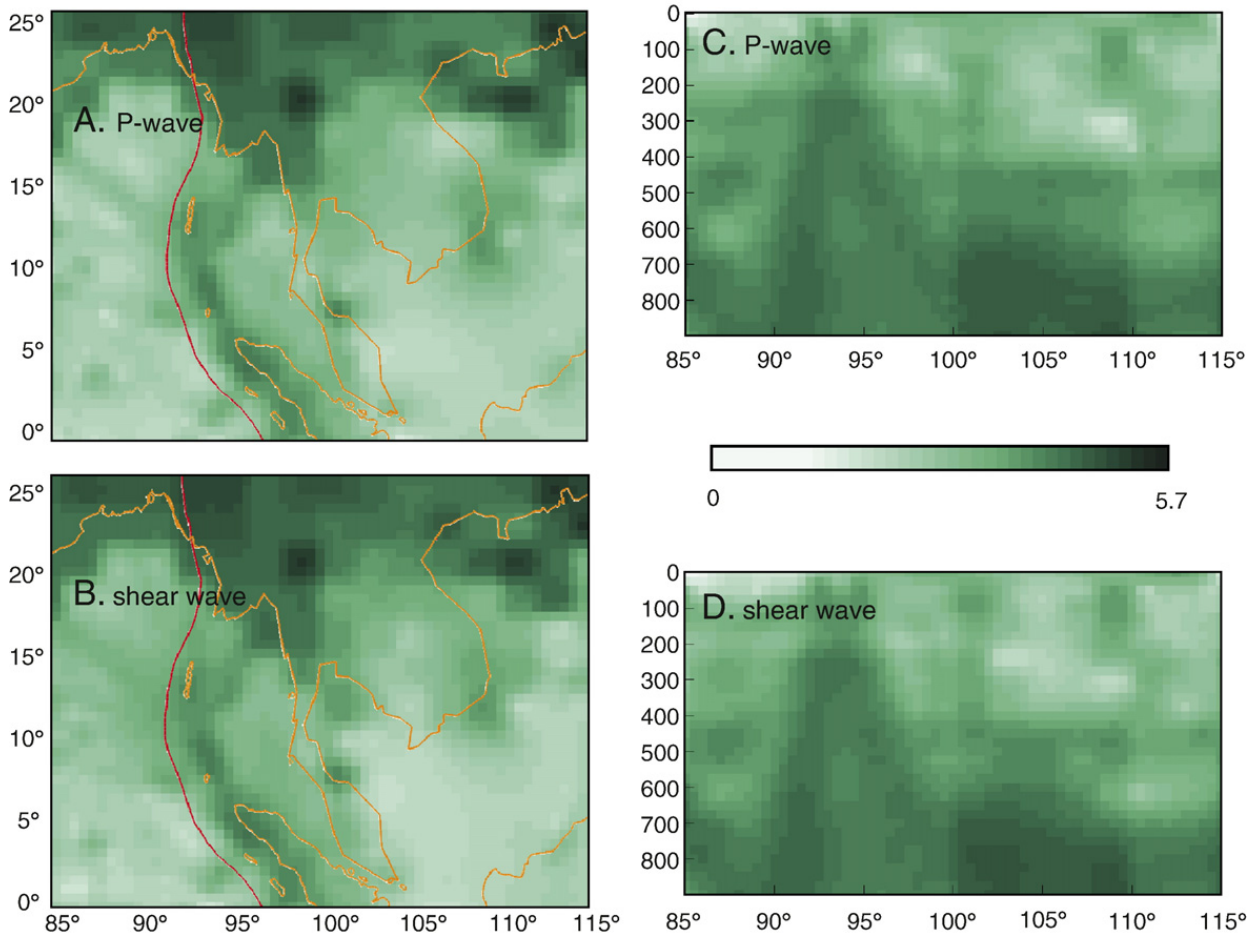

Fig. 4. Maps representing density of ray-length segments in log10 km. (A and C) P-wave and (B and D) shear-wave seismic rays illustrate the ray density in plan view sliced along 100 km depth and in cross section along A–A' shown in Figs. 1 and 3.

high Mg# andesites and dacites in subduction zones (Drummond et al., 1996). It has also been suggested to explain some of the orthopyroxene-rich peridotite xenoliths in cratonic mantle (Kelemen et al., 1998).

Another way to generate orthopyroxene-rich zones is to start from a peridotitic source (Kelemen et al., 1992). The upwelling of peridotitic mantle will generate basaltic partial melts (Fig. 6A). For a typical mantle potential temperature (~1350 °C), such melting will initially occur at high pressures (2–3 GPa ~60–90 km) and be multiply saturated in orthopyroxene, clinopyroxene, and olivine. However, as these melts ascend by porous flow through the asthenosphere, the melt will be saturated in olivine but undersaturated in pyroxenes because the olivine liquidus field expands considerably with decreasing pressure (and the pyroxene liquidus fields contract accordingly). These ascending melts will react with the surrounding peridotite by replacing pyroxenes with olivine, generating an olivine-rich (dunitic) wall–rock reaction zone. As the reaction proceeds, the melts will eventually become more Si-rich and ultimately become saturated in orthopyroxene. If these orthopyroxene-saturated melts were to intrude into the cold lithospheric mantle and cool, they would crystallize orthopyroxene (Fig. 6B). This scenario has been proposed as a process by which orthopyroxene-rich zones can be generated in mid-ocean ridge or hotspot environments (Kelemen et al., 1992). In this scenario, the generation of orthopyroxene-rich zones is favored when orthopyroxene-saturated magmas enter cold lithospheric mantle, and thus extensive orthopyroxene-rich zones would not be expected to form within typical mid-ocean ridges as there is no preexisting lithosphere in such

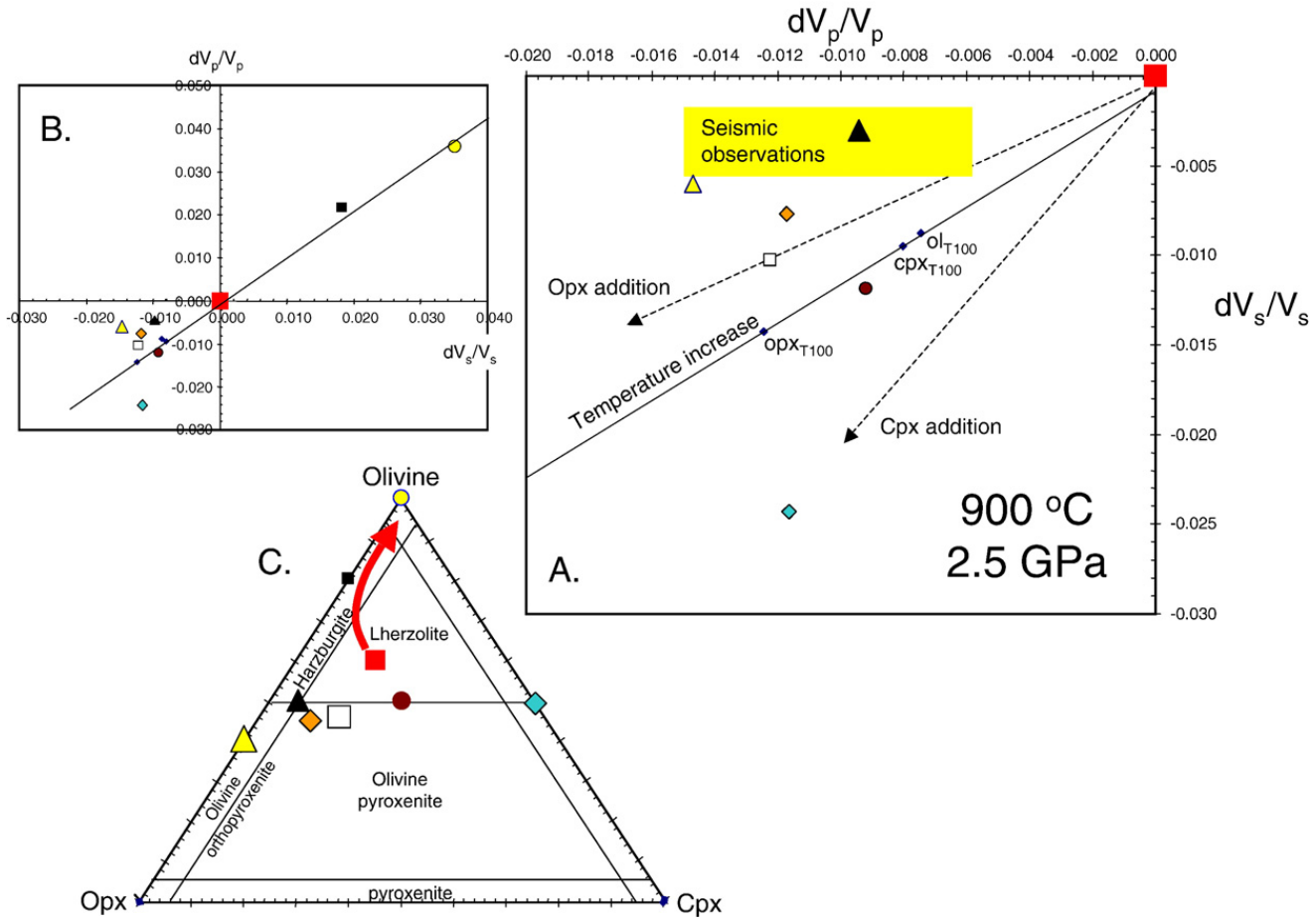

Fig. 5. A and B) Relative change in V_p versus V_s calculated at 2.5 GPa and reference temperature of 900 °C using Hacker and Abers (2004) and Lee (2003) for peridotites having modal proportions given in the ternary diagram in C. Red square in A–C represents average lherzolitic mantle. Red arrow in C represents the loci of residual peridotite compositions formed by partial melt extraction. Other symbols represent different types of orthopyroxene- (OPX) and clinopyroxene- (CPX) enriched lithologies, such as olivine orthopyroxenites, olivine pyroxenites, and olivine clinopyroxenites. Solid line in A and B represents the vector for changing temperature, taken as the regression through the three data points labeled cpx_{T100}, opx_{T100}, and ol_{T100}, which correspond to the relative decrease in velocities of each mineral due to a 100 °C increase. Using this as a reference, it can be seen that CPX-addition decreases V_s more than V_p, whereas OPX addition and CPX subtraction decrease V_p more than V_s. Yellow rectangular region represents the seismically anomalous range deduced from our tomographic results. OPX-enriched harzburgites fall within this field. (For interpretation of the references to color in this figure legend, the reader is referred to the web version of this article.)

regions. However, if the preexisting lithospheric mantle is too thick, the melting column in the asthenosphere may be too short to allow for the formation of extensive dunite channels and orthopyroxene-rich melts as reaction by-products. Thus, orthopyroxene-rich zones should not be forming in most mid-ocean ridge environments or in thick continental lithospheric mantle, but should instead be favored in regions of intermediate lithospheric thickness, such as aged oceanic lithosphere.

Of these two orthopyroxene-enrichment scenarios, the slab melting model does not seem to apply to our observations. This seismic anomaly is within the subducting oceanic slab itself, whereas the first scenario predicts the velocity anomaly to lie within the mantle wedge above a subducting slab. The second scenario is more compatible with our observations (Fig. 6C). The seismic anomaly appears to fall along the extension of the Ninetyeast Ridge after it is subducted at the Andaman arc. The exact origin of Ninetyeast is not known: it has been suggested to be the track of the Kerguelen hotspot or plume-fed ridge (Saunders et al., 1991; Sclater and Fisher, 1974; Souriau, 1981), but

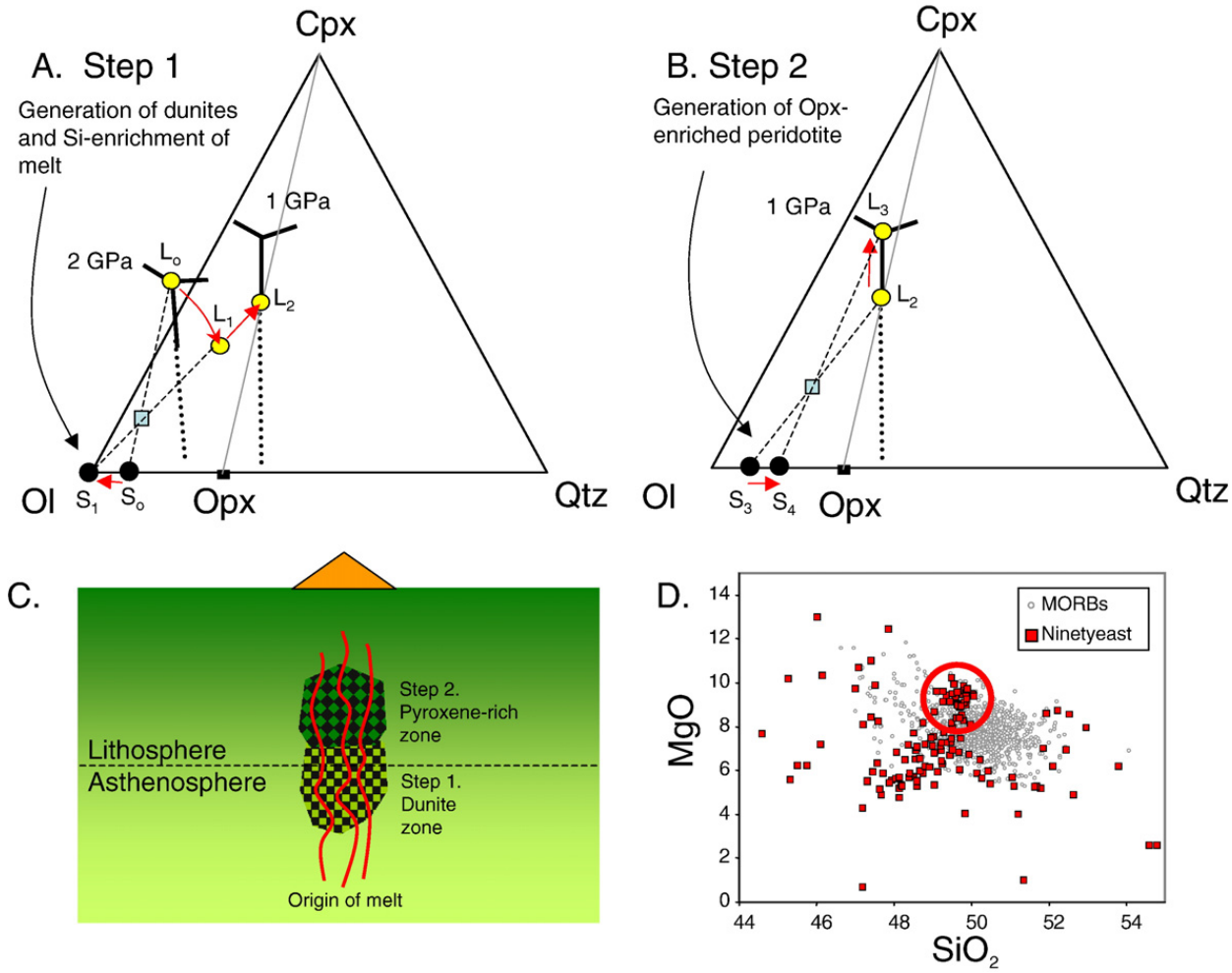

Fig. 6. A) Pseudo-quaternary phase diagram (weight %) with olivine (Ol), quartz (Qtz), and clinopyroxene (Cpx) defining the endmember components and projected from anorthite. Orthopyroxene is denoted by "Opx". Thick bold lines represent locus of multiple saturation in Ol, Opx and Cpx at 2 and 1 GPa. L_o represents the primary basalt melt composition at 2 GPa, which is in equilibrium with a solid residue having a composition denoted by S_o (solid circle); bulk composition (melt + solid residue) corresponds to a lherzolite composition (square). Decompression causes liquid L_o to become oversaturated in olivine, causing it to react with country rock (assumed to be lherzolitic) and convert pyroxene to olivine. This generates melt a silica-rich basalt L_2 in equilibrium with a dunite (S_1). B) In step 2, the silica-rich basalt L_2 cools and reacts with peridotite country rock (S_3) in the lithospheric mantle, generating an opx-enrich reaction zone or cumulate. C) Cartoon showing Steps 1 and 2 in A and B. Basaltic melt forms at depth ("origin of melt"). As it rises through the asthenosphere and base of the lithosphere, it generates olivine-rich reaction zones (dunite channels). Ensuing melts become more silicic (opx-saturated), which precipitate opx as they enter the cold lithosphere and cool. D) MgO and SiO_2 (wt. %) in mid-ocean ridge basalts (MORBs) compiled from the RidgePetDB database, and basalts from Ninetyeast Ridge. Note that some (circled region) Ninetyeast samples have high SiO_2 contents for their high MgO contents.

whatever its origin, it is the manifestation of magmatic activity beneath preexisting oceanic lithosphere since the age of the seafloor in this region is between 30 and 65 Ma. Oceanic lithosphere of such age would be 50–80 km thick and, as discussed above, could in theory favor orthopyroxene enrichment by the intrusion of orthopyroxene-saturated melts formed by reaction between hot mantle melts (presumably associated with the Kerguelen hotspot) and wall–rock peridotite in the asthenosphere.

Orthopyroxene-rich reaction zones associated with hotspot magma interaction with lithospheric mantle or melt-rock reaction in the mantle wedge have previously been suggested on the basis of petrologic observations (Kelemen et al., 1992; Wagner and Grove, 1998a). Our interpretations naturally lead to the prediction that the lithosphere underlying most of the Ninetyeast Ridge should also contain large sections of orthopyroxene-rich lithologies. While there is not enough seismic coverage in the Indian Ocean to examine the rest of the Ninetyeast Ridge, we can instead examine the major element compositions of magmas erupted along Ninetyeast. Using the data of Hekinian (1974) and Frey et al. (1991), we find that the SiO_2 contents (at a given MgO) of the Ninetyeast Ridge dredge and drill core samples are virtually identical to those of mid-ocean ridge basalts (MORBs) (Fig. 6D). SiO_2 content is roughly inversely proportional to the average pressure of melting (Albarède, 1992). Thus, because the average pressure of melting for Ninetyeast Ridge basalts should be higher due to the presence of a preexisting lithospheric cap that the magmas must rise through, we would expect such basalts to have slightly lower SiO_2 contents than MORBs. However, the similar SiO_2 contents between Ninetyeast Ridge basalts and MORB suggest that the Ninetyeast Ridge basalts last equilibrated with an anomalously Si-rich lithology, and if so, this would be consistent with an orthopyroxene-enriched reaction zone.

6. Conclusions

The unusual seismic anomaly imaged within the subducting Indo-Australian plate depicts a negative perturbation in both P-wave and bulk-sound speed, but little change in S-wave speed. The unique characteristics of this anomaly allow us to exclude the effects of temperature, density, and along arc morphological variations in the slab structure as possible explanations for its existence. The position of the Ninetyeast Ridge at the Sumatra–Andaman arc and its relation to the anomalous velocities at depth (60–160 km) suggest that the plume-fed ridge has played an essential role in the formulation of this anomaly. Previous papers have linked seamount chains and topographic highs to changes in morphology and physical properties of subducting slabs (Miller et al., 2005, 2004), and further suggested that the presence of subducted oceanic plateaus can affect the chemical "budget" of the deep mantle (Albarede and van der Hilst, 2002). Other papers have suggested compositional anomalies in the mantle wedge above subduction zones (Brudzinski and Chen, 2003; Chen and Brudzinski, 2001; Wagner et al., 2005), but here we suggest that the linear topographic high, the Ninetyeast Ridge, has changed the physical properties of the subducted slab through chemical modification. These chemical modifications, identified as a possible large orthopyroxene-rich zone, may be the first to be identified as anomalous seismic velocities within this depth range. We propose that hotspot magma interacting with lithospheric mantle could lead to orthopyroxene enrichment. The intrusion of orthopyroxene-saturated melts could have been formed by the reaction between hot mantle melts and wall–rock peridotite in the asthenosphere. Evidence for such extensive chemical modification has not yet been observed seismically. We have fortunately been afforded the unique opportunity to image chemical modification as the ridge being subducted is now extinct, therefore not obscured seismically by melt, and because the resolution of the tomographic images along the Sumatra–Andaman arc is of high-quality due to the large number of earthquakes and sufficient number of seismic stations in the area. As digital seismicity catalogues continue to grow and the number of seismometers along subduction zones increase, other regions such as subduction along the Central American, South American, New Hebrides, and the Kurile trench will be analyzed for unusual upper mantle anomalies related to subduction of ridges or oceanic plateaus.

Acknowledgments

We would like to thank the Rice University Loony Noons participants for feedback, Alexei Gorbatov, Fenglin Niu, Brian Kennett, NSF, NSERC postdoctoral fellowship awards, the Packard foundation, and Matt Fouch and another anonymous reviewer for their comments and suggestions to improve the manuscript.

References

Albarède, F., 1992. How deep do common basaltic magmas form and differentiate? J. Geophys. Res. 97, 10997–11009.

Albarede, F., van der Hilst, R.D., 2002. Zoned mantle convection. Philos. Trans. R. Soc. Lond. A. A360, 2569–2592.

Bass, J.D., 1995. Elasticity of minerals, glasses, and melts, Mineral Physics and Crystallography. Am. Geophys. Union 45–63.

Boyd, F.R., 1989. Compositional distinction between oceanic and cratonic lithosphere. Earth Planet. Sci. Lett. 96, 15–26.

Brudzinski, M.R., Chen, W.-P., 2003. A petrologic anomaly accompanying outboard earthquakes beneath Fiji-Tonga: corresponding evidence from broadband P and S waveforms. J. Geophys. Res. 108. doi:10.1029/2002JB002012.

Chai, M., Brown, J.M., Slutsky, L.J., 1997. The elastic constants of an aluminous orthopyroxene to 12.5 GPa. J. Geophys. Res. 102, 14779–14785.

Chen, W.-P., Brudzinski, M.R., 2001. Evidence for a large-scale remnant of subducted lithosphere beneath Fiji. Science 292, 2475–2479.

Drummond, M.S., Defant, M.J., Kepezhinskas, P.K., 1996. Petrogenesis of slab-derived trondhjemite–tonalite–dacite/adakite magmas. Trans. Roy. Soc. Edinburgh 87, 205–215.

Engdahl, E.R., van der Hilst, R.D., Buland, R., 1998. Global teleseismic earthquake relocation with improved travel times and procedures for depth determination. Bull. Seismol. Soc.Am. 88, 722–743.

Fouch, M.J., James, D.E., VanDecar, J.C., van der Lee, S., 2004. Mantle seismic structure beneath the Kaapvaal and Zimbabwe Cratons. S. Afr. J. Geol. 107, 33–44.

Frey, F.A., Jones, W.B., Davies, H., Weis, D., 1991. Geochemical and petrologic data for basalts from sites 756, 757, and 758: implications for the origin and evolution of Ninetyeast Ridge. Proc. Ocean Drill. Program, Sci. res. 121, 611–659.

Gorbatov, A., Kennett, B.L.N., 2003. Joint bulk-sound and shear tomography for western Pacific subduction zones. Earth Planet. Sci. Lett. 210, 527–543.

Hacker, B.R., Abers, G.A., 2004. Subduction factory 3: an Excel worksheet and macro for calculating the densities, seismic wave speeds, and H2O contents of minerals and rocks at pressure and temperature. Geochem. Geophys. Geosys. 5. doi:10.1029/2003GC000614.

Hekinian, R., 1974. Petrology of igneous rocks from Leg 22 in the northeastern Indian Ocean. Initial Reports of the Deep Sea Drilling Project, 22, pp. 413–447.

Horodyskyj, U., Lee, C.-T.A., Ducea, M.N., 2007. Similarities between Archean high MgO eclogites and Phanerozoic arc-eclogite cumulates and the role of arcs in Archean continent formation. Earth Planet. Sci. Lett. 256, 510–520.

James, D.E., Fouch, M.J., VanDecar, J.C., van der Lee, S., 2001. Tectospheric structure beneath southern Africa. Geophys. Res. Lett. 28, 2485–2488.

Kelemen, P.B., 1995. Genesis of high Mg# andesites and the continental crust. Contrib. Mineral. Petrol. 120, 1–19.

Kelemen, P.B., Dick, H.J.B., Quick, J.E., 1992. Formation of harzburgite by pervasive melt/rock reaction in the upper mantle. Nature 358, 635–641.

Kelemen, P.B., Hart, S.R., Bernstein, S., 1998. Silica enrichment in the continental upper mantle via melt/rock reaction. Earth Planet. Sci. Lett. 164, 387–406.

Kennett, B.L.N., Engdahl, E.R., Buland, R., 1995. Constraints on seismic velocities in the Earth from traveltimes. Geophys. J. Int. 122, 108–124.

Kennett, B.L.N., Widiyantoro, S., van der Hilst, R.D., 1998. Joint seismic tomography for bulk sound and shear wave speed in the Earth's mantle. J. Geophys. Res. 103, 12,469–412,493.

Koketsu, K., Sekine, S., 1998. Psuedo-bending method for three-dimensional seismic ray tracing in a spherical Earth with discontinuities. Geophys. J. Int. 132, 339–346.

Lee, C.-T.A., 2003. Compositional variation of density and seismic velocities in natural peridotites at STP conditions: implications for seismic imaging of compositional heterogeneities in the upper mantle. J. Geophys. Res. 108, 2441. doi:10.1029/2003JB002413.

Liu, Y., Shan, G., Lee, C.-T.A., Hu, S., Liu, X., Yuan, H., 2005. Melt–peridotite interactions: links between garnet pyroxenite and high-Mg# signature of continental crust. Earth Planet. Sci. Lett. 234, 39–57.

Miller, M.S., Kennett, B.L.N., Lister, G.S., 2004. Imaging changes in morphology, geometry, and physical properties of the subducting Pacific plate along the Izu–Bonin–Mariana arc. Earth Planet. Sci. Lett. 224, 363–370.

Miller, M.S., Gorbatov, A., Kennett, B.L.N., 2005. Heterogeneity within the subducting Pacific slab beneath the Izu–Bonin–Mariana arc: Evidence from tomography using 3D ray tracing inversion techniques. Earth Planet. Sci. Lett. 235, 331–342.

Miller, M.S., Gorbatov, A., Kennett, B.L.N., 2006. Three-dimensional visualization of a near-vertical slab tear beneath the southern Mariana arc. Geochem. Geophys. Geosys. 7. doi:10.1029/2005GC001110.

Müller, R.D., Roest, W.R., Royer, J.-Y., Gahagan, L.M., Sclater, J.G., 1997. Digital isochrons of the world's ocean floor. J. Geophys. Res. 102, 3211–3214.

Rapp, R.P., Shimizu, N., Norman, M.D., Applegate, G.S., 1999. Reaction between slab-derived melts and peridotite in the mantle wedge: experimental constraints at 3.8 GPa. Chem. Geol. 160, 335–356.

Saunders, A.D., Storey, M., Gibson, I.L., Leat, P., Hergt, J., Thompson, R.N., 1991. Chemical and isotropic constraints on the origin of basalts from Ninetyeast Ridge, Indian Ocean: results from DSDP legs 22 and 26 and ODP leg 1211. In: Weissel, J., Perice, J., Taylor, E., Alt, J. (Eds.), Proceedings of the Ocean Drilling Program, Scientific Results. Ocean Drilling Program, College Station, TX, pp. 559–590.

Sclater, J.G., Fisher, R.L., 1974. Evolution of the east central Indian Ocean, with emphasis on the tectonic setting of the Ninetyeast ridge. Geol. Soc. Amer. Bull. 85, 683–702.

Souriau, A., 1981. The upper mantle beneath Ninetyeast Ridge and Broken Ridge, Indian Ocean, from surface waves. Geophys. J. Int. 67, 359–374.

Wagner, T.P., Grove, M., 1998a. Melt/harzburgite reaction in the petrogenesis of tholeiitic maga from Kilauea volcano, Hawaii. Contrib. Mineral. Petrol. 131, 1–12.

Wagner, T.P., Grove, M., 1998b. Melt/harzburgite reaction in the petrogenesis of tholeiitic maga from Kilauea volcano, Hawaii. Contrib. Mineral. Petrol. 131, 1–12.

Wagner, T.P., Beck, S.L., Zandt, G., 2005. Upper mantle structure in the south central Chilean subduction zone (30° to 36 °S). J. Geophys. Res. 110. doi:10.1029/2004JB003238.